Paper: ASAT-17-140-MO

17th International Conference on
AEROSPACE SCIENCES & AVIATION TECHNOLOGY,
ASAT - 17 – April 11 - 13, 2017, E-Mail: asat@mtc.edu.eg
Military Technical College, Kobry Elkobbah, Cairo, Egypt
Tel: +(202) 24025292 – 24036138, Fax: +(202) 22621908

Modeling and Simulation of Telescopic Rotary Crane

Ahmed Y. AbdelHamid[*], Mohamed H. Mabrouk[†], Hosam A. AbdelKader [‡]

Abstract: Rotary cranes are widely used in construction operations to load and unload materials in field. However, the efficiency of cranes loading operation could be limited due to the crane's slewing rotational motion that generates undesirable two-dimensional load sway. Various attempts of load sway control have been proposed to reduce the dependence on human operator's skills as well as to increase their safety. This paper presents a dynamic model for a telescopic rotary crane (TRC) to help in developing a load sway control method for the system. Velocity trajectory patterns such as S-curve pattern, cubic path pattern, quantic path pattern and zero jerk path pattern are generated by solving the algebraic equations numerically. The validation of the developed model and used operational parameters is demonstrated by comparing the model results to published numerical results and virtual simulation results using Sim-Mechanics toolbox of MATLAB®.

Keywords: Hoisting machinery, modeling and simulation of dynamic systems, trajectory generation.

1. Introduction

Rotary cranes are widely used to transport heavy loads and hazardous materials in various environments, such as shipyards, factories, railway yards, nuclear installations, and construction sites. However, the efficiency of cranes during the loading / unloading operations could be limited because of the slewing rotational motion of a rotary crane that generates undesirable two-dimensional load sway. Skilled crane operators are required to manually control boom operation based on their experiences in arresting load sway immediately at a desired position that is difficult to achieve. Moreover, failures of crane control may cause accidents of people injure and/or damage surroundings.

Over the last decades, researchers have built systems models, which leads to proposed controllers for suppressing load sway caused by horizontal boom motion to reduce the dependence on human operator's skills and to increase the loading / unloading operations' safety. Those controllers can be branched into two main categories. Open-loop trajectory generation controllers for the crane's motion that can suppress load sway with-out requiring load sway information [1-9] , and closed loop controllers that use real time information measured by sensors to suppress load sway [1-13].

However, numerous control approaches dealing with sway free transportation of crane loads were proposed, few attempts focus on the rotary crane. Recently most research about the anti-sway systems focused on gantry and overhead cranes [14].

[*] Egyptian Armed Forces, Egypt; *ayahia@mtc.edu.eg*
[†] Egyptian Armed Forces, Egypt; *mmabrouk@mtc.edu.eg*
[‡] Egyptian Armed Forces, Egypt; *hosamabdelkader@mtc.edu.eg.*

The major objective of the anti-sway control method for a telescopic rotary crane is the damping of the load sway and tracking of a reference trajectory of the load during its transfer operation. The main challenge for the realization of such a control concept is the measurement of the rope angles, as well as, the coupling of the moving axes due to centrifugal forces.
Due to the mentioned challenges, there are few control concepts in the literature, which have proven applicable in practice Also, the anti-sway and trajectory tracking problem for rotary crane is defined only in theory [6].while their implementations have never exceeded model scaled attempted [15].
This paper focuses on developing a dynamic model of the telescopic rotary crane (TRC) that can help to design a reliable controller for the system. The model aims to predict the correct values of the swaying angles to use it as a feedback signal to suppress the residual load sway as possible by using different control methods. The verification of the TRC model is achieved
by applying different reference trajectories and different inputs such as (damping ratio ,friction coefficient ,vertical boom angle,…etc.) to the developed Sim-Mechanics model and compare the results of the two swaying angles with the difference inputs., A simple dynamics model is proposed for open-loop residual load sway suppression. In Ref [6], a simple model considering only centrifugal force as a nonlinear effect for feedback control is presented.
The efficiency of the proposed TRC model can be checked by developing simple S-curve trajectory, cubic path pattern, quantic path pattern and zero jerk path pattern for horizontal boom motion. Then the generated trajectory is compared with that of existing method using numerical simulation results and virtual simulation results using Sim-Mechanics toolbox of MATLAB® are conducted under several motion conditions.

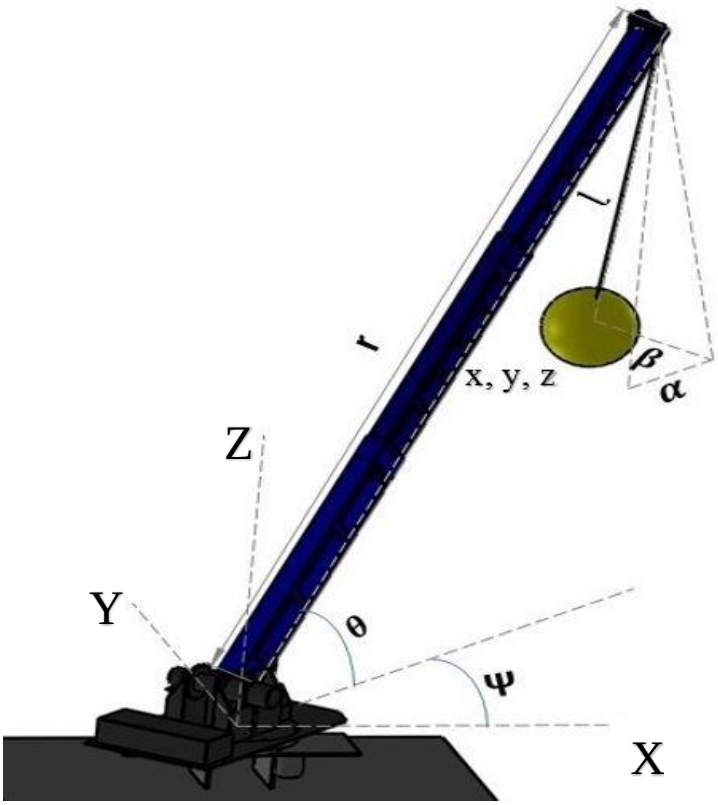

Fig. 1. Schematic model of Telescopic rotary crane.

2. Mathematical Model Dynamics and Verification

A dynamical model of a three-dimensional boom crane whose schematic model is shown in Fig. 1 is derived. The boom crane can rotate around the vertical axis z and move the boom in order to vary the outreach of the load. The typical spherical load oscillations, which are excited

by the crane's slewing and luffing motion, are described by the rope angles projected onto the tangential and radial plane (***α*** and***β***. respectively). ***θ*** and ***ψ*** are the vertical and horizontal (slewing) angles of the boom, respectively. **l** and ***r*** denote the lengths of the rope and boom, respectively. (**x, y, z**) denotes the Cartesian coordinate position of the load. In order to obtain a sufficient representation of the dynamical crane behavior, a model of the load pendulation is derived using the method of Euler–Lagrange. Solving the Euler-Lagrange equations leads to the exact equations of motion of the spherical load pendulation. The complexity of the dynamical model can be solvable by making the following assumptions:

1. The body of the crane is regarded as a rigid body.
2. The load is regarded as a point mass.
3. The mass and flexibility of the rope are neglected.

With these definitions, the x-, y- and z-components of the payload position are given by:

$$\begin{pmatrix} \mathrm{x} \\ \mathrm{y} \\ \mathrm{z} \end{pmatrix} = \begin{pmatrix} r\ \cos\theta\cos\varphi \\ r\ \cos\theta\ \sin\varphi \\ r\ \sin\theta \end{pmatrix} + \begin{pmatrix} l\left(\cos\beta\sin\alpha\ \cos\varphi - \sin\beta\sin\varphi\right) \\ l\left(\cos\beta\sin\alpha\ \sin\varphi + \sin\beta\cos\varphi\right) \\ -l\left(\cos\beta\cos\alpha\right) \end{pmatrix} \tag{1}$$

The kinetic energy *T* and potential energy *U* of the load are defined as follows:

$$T = \frac{1}{2} m\left(\dot{\mathrm{x}}^2 + \dot{\mathrm{y}}^2 + \dot{\mathrm{z}}^2\right) \tag{2}$$

$$U = m.g.\mathrm{z} \tag{3}$$

The equations of motion can be derived by introducing the Lagrangian function, which defined as:

$$L = T - U \tag{4}$$

$$\begin{aligned} L = \frac{m}{2}\Big(&-\dot{\psi}^2\cos(\beta)^2\cos(\alpha)^2 l^2 + 2\cos(\theta)\dot{\psi}^2\sin(\alpha)\cos(\beta) lr + \dot{\psi}^2 l^2 \\ &+\cos(\beta)^2\dot{\alpha}^2 l^2 + 2\dot{\psi}\,\dot{\beta}\sin(\alpha) l^2 + 2gl\cos(\beta)\cos(\alpha)) + \cos(\theta)^2\dot{\psi}^2 r^2 \\ &+\dot{\beta}^2 l^2 - 2\dot{\psi}\sin(\beta)\cos(\beta)\dot{\alpha}\cos(\alpha) l^2 + 2\cos(\theta)\dot{\psi}\,\dot{\beta}\,\cos(\beta) lr \end{aligned} \tag{5}$$

The Euler-Lagrange equations are given by:

$$\frac{d}{dt}\left(\frac{\partial L}{\partial \dot{q}_i}\right) - \frac{\partial L}{\partial q_i} = Q_i \tag{6}$$

where, q_i are the generalized coordinates, where $q_0 = \alpha$ and $q_1 = \beta$.the term $Q_i$represents the generalized forces, and is equal to the sum of external forces and torques acting on the system. Compensation from the Lagrangian eq. (5) into eq. (6), the desired equations of motion are obtained. The first equation, describing the rotational motion, is derived as follows:

$$\frac{d}{dt}\left(\frac{\partial L}{\partial \dot{\alpha}}\right)-\frac{\partial L}{\partial \alpha}=0 \tag{7}$$

$$\begin{aligned}&\cos(\beta)\cos(\alpha)\dot{\psi}^2\sin(\alpha)l+2\cos(\beta)\cos(\alpha)\dot{\psi}\,\dot{\beta}\,l+\cos(\alpha)\dot{\psi}^2\cos(\theta)r\\&+\ddot{\psi}\sin(\beta)\cos(\alpha)l+2\sin(\beta)\,\dot{\beta}\,\dot{\alpha}\,l-\cos(\beta)\ddot{\alpha}l-\sin(\alpha)g=0\end{aligned} \tag{8}$$

$$\frac{d}{dt}\left(\frac{\partial L}{\partial \dot{\beta}}\right)-\frac{\partial L}{\partial \beta}=0 \tag{9}$$

$$\begin{aligned}&-\sin(\beta)\cos(\beta)\cos(\alpha)^2\dot{\psi}^2l+\sin(\beta)\dot{\psi}^2\cos(\theta)\sin(\alpha)r+\ddot{\psi}\,l\sin(\alpha)\\&+2\cos(\beta)^2\cos(\alpha)\dot{\psi}\,\dot{\alpha}\,l+\sin(\beta)\cos(\beta)\,\dot{\alpha}^2l+\ddot{\psi}\,\cos(\beta)\cos(\theta)r\\&+\sin(\beta)\cos(\alpha)g+\ddot{\beta}l=0\end{aligned} \tag{10}$$

By solving equations (9. 10) together for getting the variables$\ddot{\alpha},\ddot{\beta}$.

$$\begin{aligned}\ddot{\alpha}=&\frac{1}{l\cos(\beta)}(\cos(\beta)\cos(\alpha)\dot{\psi}^2\sin(\alpha)l+2\cos(\beta)\cos(\alpha)\dot{\psi}\,\dot{\beta}\,l\\&+2\sin(\beta)\,\dot{\beta}\,\dot{\alpha}\,l+\cos(\alpha)\dot{\psi}^2\cos(\theta)r+\ddot{\psi}\sin(\beta)\cos(\alpha)l-\sin(\alpha)g)\end{aligned} \tag{11}$$

$$\begin{aligned}\ddot{\beta}=&\frac{1}{l}(-2\cos(\beta)^2\cos(\alpha)\dot{\psi}\,\dot{\alpha}\,l-\sin(\beta)\cos(\beta)\dot{\alpha}^2l-\ddot{\psi}\cos(\beta)\cos(\theta)r\\&+\sin(\beta)\cos(\beta)\cos(\alpha)^2\dot{\psi}^2l-\sin(\beta)\dot{\psi}^2\cos(\theta)\sin(\alpha)r\\&-\sin(\beta)\cos(\alpha)g-\ddot{\psi}l\sin(\alpha))\end{aligned} \tag{12}$$

where g denotes the gravitational acceleration. Because Eqs. (11) and (12) of the crane model are complicated, a simple model is needed for controller design. First of all as the sway angles $\boldsymbol{\alpha}$ and $\boldsymbol{\beta}$ have a small magnitude these assumptions can be considered ($\sin\alpha\cong\alpha$, $\cos\alpha\cong 1, \sin\beta\cong\beta$ $\cos\beta\cong 1$)

$$\ddot{\alpha}=\frac{1}{l}(\dot{\psi}^2\alpha l+2\dot{\psi}\,\dot{\beta}\,l+2\beta\,\dot{\beta}\,\dot{\alpha}\,l+\dot{\psi}^2\cos(\theta)r+\ddot{\psi}\beta l-\alpha\,g) \tag{13}$$

$$\ddot{\beta}=\frac{1}{l}(-2\dot{\psi}\dot{\alpha}l-\beta\dot{\alpha}^2l-\ddot{\psi}\cos(\theta)r+\beta\,\dot{\psi}^2l-\beta\dot{\psi}^2\cos(\theta)\alpha\,r-\beta g-\ddot{\psi}\alpha\,l) \tag{14}$$

Ref. [6] presented a verifying model of a rotary crane that includes only a centrifugal force term for feedback control to achieve load sway suppression by using only horizontal boom motion. However, in this study, a more precise model is needed for achieving open-loop control without measuring the load sway. Because the centrifugal force and Coriolis force caused by horizontal boom motion, and gravitational force affect two dimensional load sway significantly, to derive

the trajectory by numerical calculation easily, all the terms in Eqs. (1) and (2) are linearized except some centrifugal, Coriolis, and gravitational force terms.by assuming that (($\boldsymbol{\alpha}, \dot{\boldsymbol{\alpha}}, \boldsymbol{\beta}$ and$\dot{\boldsymbol{\beta}}$) are small such that $\dot{\boldsymbol{\alpha}}$ and $\dot{\boldsymbol{\beta}} \cong 0, \boldsymbol{\alpha} * \boldsymbol{\beta} \cong 0, \dot{\boldsymbol{\alpha}}^{\mathbf{2}} * \boldsymbol{\beta}$ and $\boldsymbol{\alpha} * \dot{\boldsymbol{\beta}}^{\mathbf{2}} \cong 0, \dot{\boldsymbol{\alpha}} * \dot{\boldsymbol{\psi}} \cong 0, \boldsymbol{\alpha} * \ddot{\boldsymbol{\psi}}$and $\boldsymbol{\beta} * \ddot{\boldsymbol{\psi}} \cong 0$) are satisfied.

$$\ddot{\alpha} = (2\dot{\psi}\,\dot{\beta} + \frac{\cos(\theta) r}{l}\dot{\psi}^2 - \frac{g}{l}\,\alpha) \tag{15}$$

$$\ddot{\beta} = (\frac{\cos(\theta) r}{l}\ddot{\psi} - \frac{g}{l}\beta) \tag{16}$$

Considering Eqs. (15) and (16) at the following simple dynamical model of rotary crane:

$$\ddot{\alpha} + \omega_n{}^2\,\alpha = b\dot{\psi}^2 \tag{17}$$

$$\ddot{\beta} + \omega_n{}^2\,\beta = -b\ddot{\psi} \tag{18}$$

where,$\omega_n = \sqrt{(g/l)}$ and $b = (\frac{r\cos\theta}{l})$.

Because the load sway $\boldsymbol{\beta}$ can be controlled directly by the control input $\ddot{\psi}$ and its effect is significant, the Coriolis force term is not included in Eq. (18). Similar to the most existing studies, Eqs. (17) and (18) do not include viscous friction effects, although they can be included if necessary

Verification of simple model

Because analytical validation of the model in Eqs. (17) and (18) is difficult; a simple model is derived in Eqs. (20) and (21) then a comparative simulations with the parameters of the crane system shown in Table 1 using a step reference trajectory are conducted based on the model in Eqs. (17) and (18) (TRC model 1), the model used by N. Uchiyama in [6] (model 2), and the (Sim-Mechanics model) which will be described in section 3 later for verifying the validity of the proposed TRC model. A simulation in which the reference trajectory for the horizontal boom motion is given as follows:

$$r = \theta_f \qquad t \in [0, T_f\,] \tag{19}$$

where θ_f is the final angle, and was set to 45 deg, and T_f is the final time

Table 1 parameter of rotary crane

r [m].	0.65	θ[deg]	45
l [m].	0.4	g [rad/sec^2]	9.81
ψ_f[deg]	45	T_f [sec]	10

Simulation results for ψ_f= 45 deg is shown in Fig. 2. Although the same results are almost obtained for α in Fig. 2, only the (TRC model) provides the similar profile with that of the (Sim-Mechanics model), As there are slight different profiles are obtained between the (TRC model) and the (Sim-Mechanics model), much better results are confirmed compared to the (model 2) the errors in load sway angles are increased when the angles ψ is increased. The error in load

sway obtained based on the (TRC model) is considerably smaller than that based on the (model 2). The (TRC model) provides better performance than the (model)

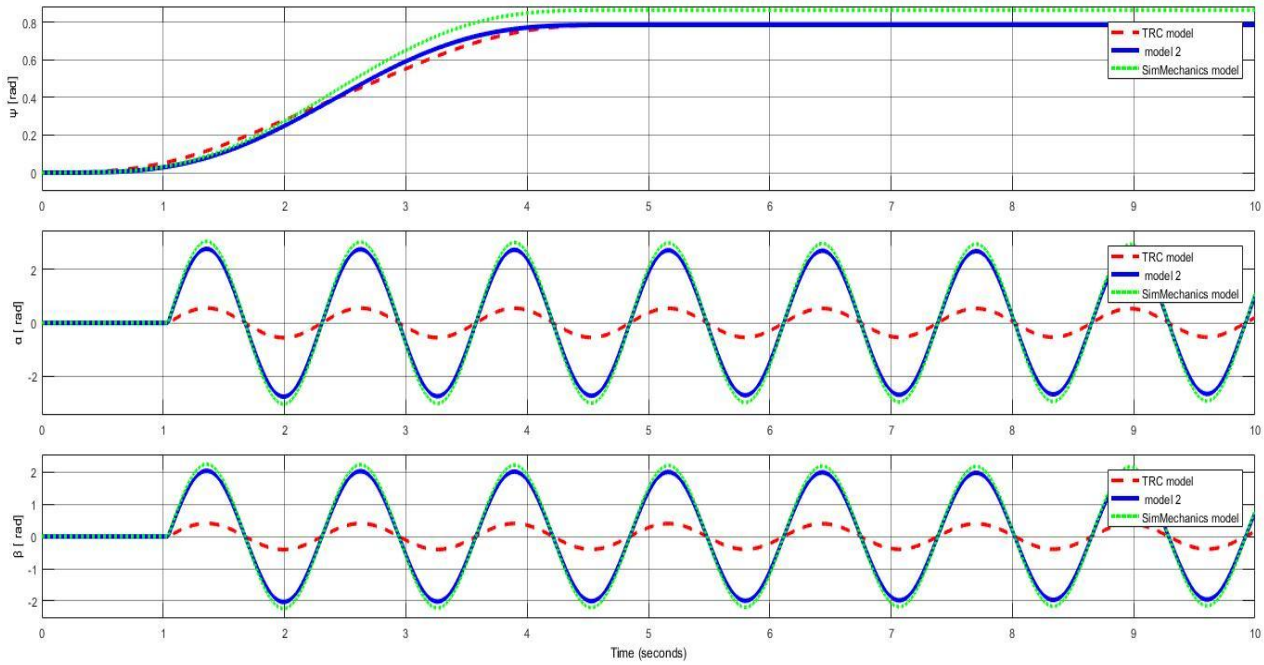

Fig. 2. Comparative simulation results of load sway angles at (ψ_f=0.7853[rad])

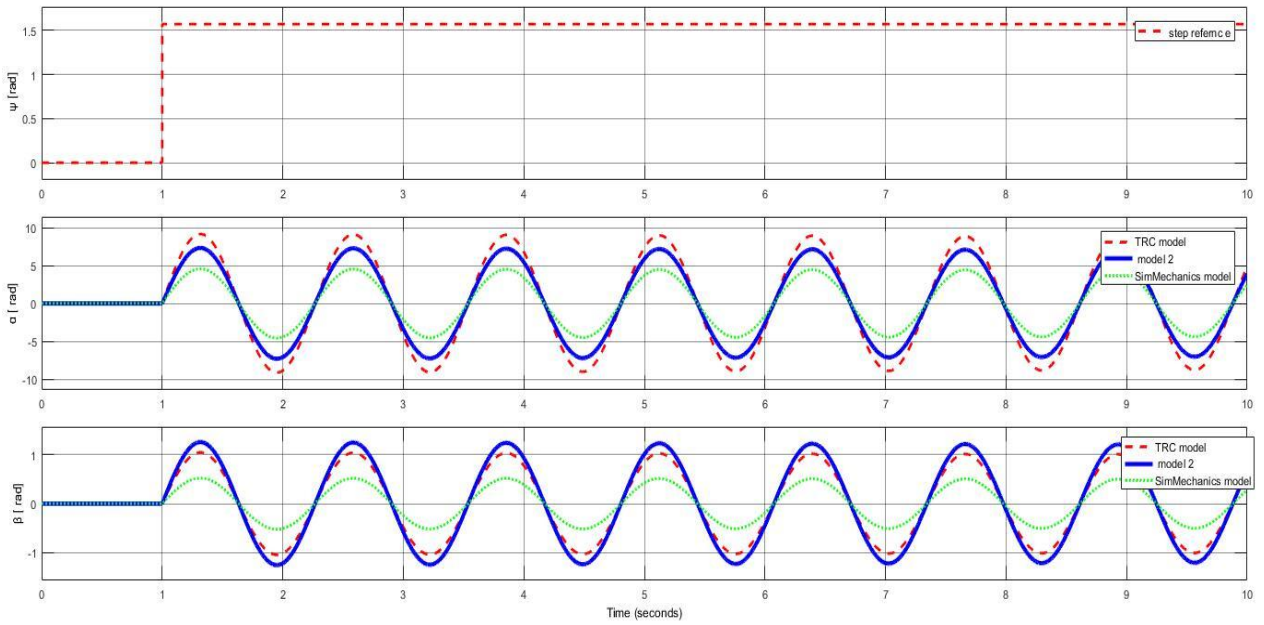

Fig. 3. Comparative simulation results of load sway angles at (ψ_f=1.5706[rad])

Simulation with Sim-Mechanics

Sim-Mechanics is a MATLAB® toolbox that enable importing CAD model from a CAD environment to the Simulink environment as blocks of links connected by joints. In addition to this, Simulink provides users with a tool to specify bodies and their mass properties [16, 17], their possible motions, kinematic constraints, coordinate systems and the means of initiating and measuring motions. This makes it easier to do the analytical modeling without involving in a complex modeling process. Firstly, a CAD model needs to be built. SOLIDWORKS® is used as a suitable platform for this reason as shown in Fig. 5. Secondly, this CAD model is imported

to MATLAB® Simulink as an .XML file by the aid of Sim-Mechanics toolbox as shown in Fig. 8.

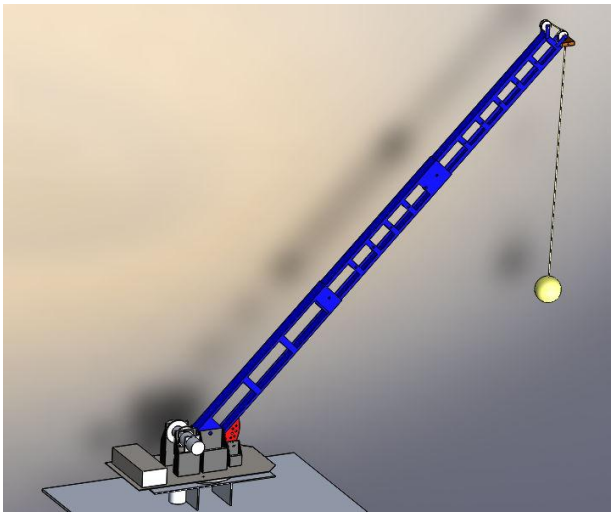

Fig. 8 Telescopic rotary crane CAD model

The produced model consists of body blocks that connected together with joint blocks and fixed from the base to the ground. Every joint can be drive with one of two block options; generalized forces actuation, and motion actuation. The dynamic parameters like mass, inertia, and CG position of any part transfer from CAD model to the Simulink body blocks. In addition, position, velocity, and acceleration measurements can be produced using joint or body sensor. The required measurements can be chosen from the sensor block.

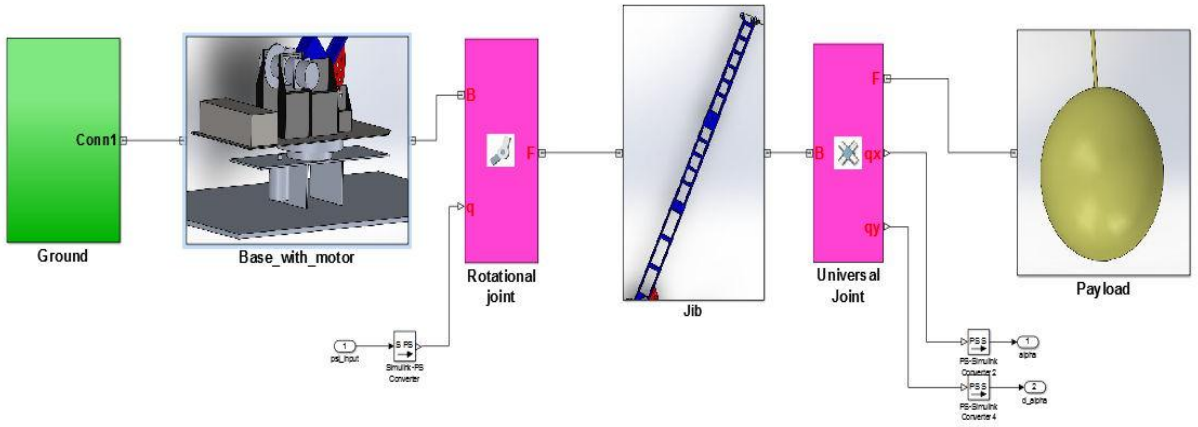

Fig. 9 Sim-Mechanics model of Telescopic rotary crane

Finally, the overall crane Simulink model presented as illustrated in Fig. 7. It is seen that this model consists of five main blocks; desired input block, trajectory generation block, crane model block, measurements block, and root mean square error block.

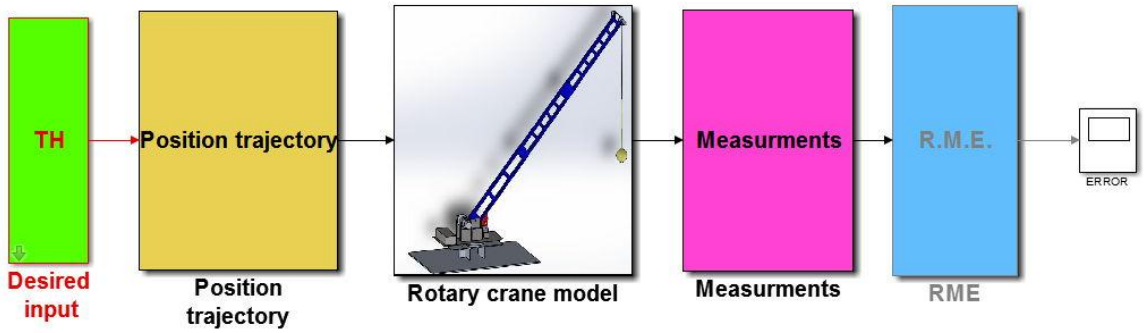

Fig. 10Simulink model of Telescopic rotary crane

Fig.8 shows the window of virtual simulation of Sim-Mechanics toolbox and the 3D animation of the crane motion with the spherical pendulum swing.

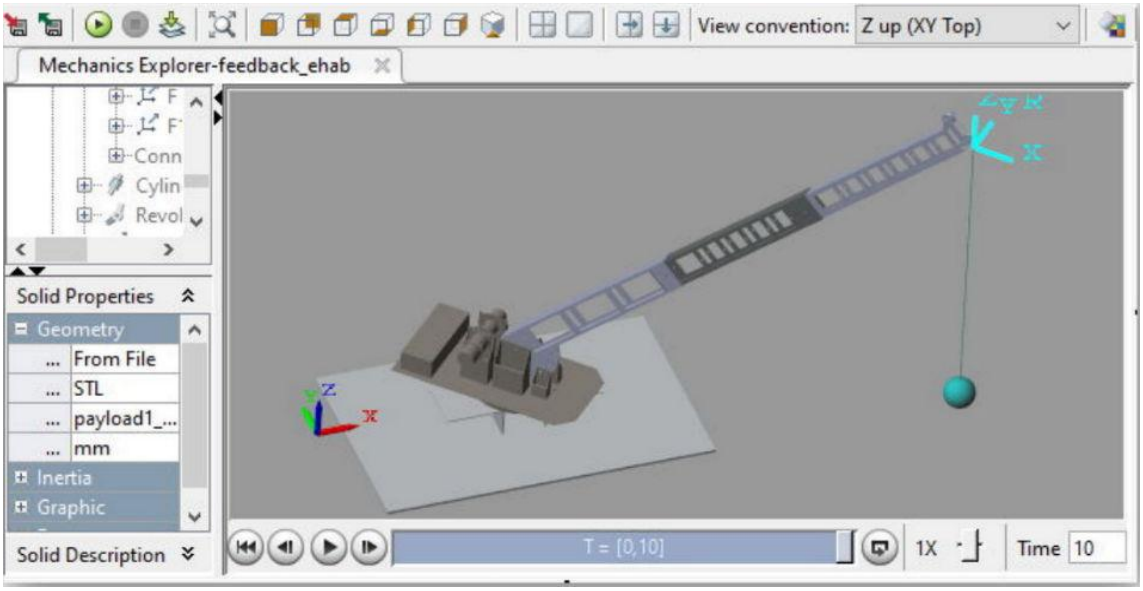

Fig. 11 3D simulation of Telescopic rotary crane

3. Trajectory Generation and Control

The main purpose of this section is to find a trajectory that connects an initial and final configuration while satisfying other specified constraints at the terminal points (e.g., velocity and/or acceleration constraints)[18].

3.1. Cubic Polynomial Trajectory

One way to generate a smooth curve is by a polynomial function of time. To satisfy a path with four constraints, a polynomial with four independent coefficients is required. Thus, a cubic trajectory is considered as following;
For position:

$$\psi(t) = a_0 + a_1 t + a_2 t^2 + a_3 t^3 \tag{19}$$

For velocity:

$$\ddot{\psi}(t) = a_1 + 2a_2 t \quad + 3a_3 t^2 \tag{20}$$

By using MATLAB, values of (a_0, a_1, a_2, a_3) can be determined, where the shape of the trajectory (position, velocity, acceleration) curves of a cubic path starts at t_0=0 [sec] with ψ_0=0 [deg] and initial Velocity $\dot{\psi}_0$ =0 [deg/sec], and end at t_f=10 [sec] with ψ_f=45 [deg] (ψ_f=0.7853[rad]) and final velocity $\dot{\psi}_f$=0 deg/sec shown in Fig. 2

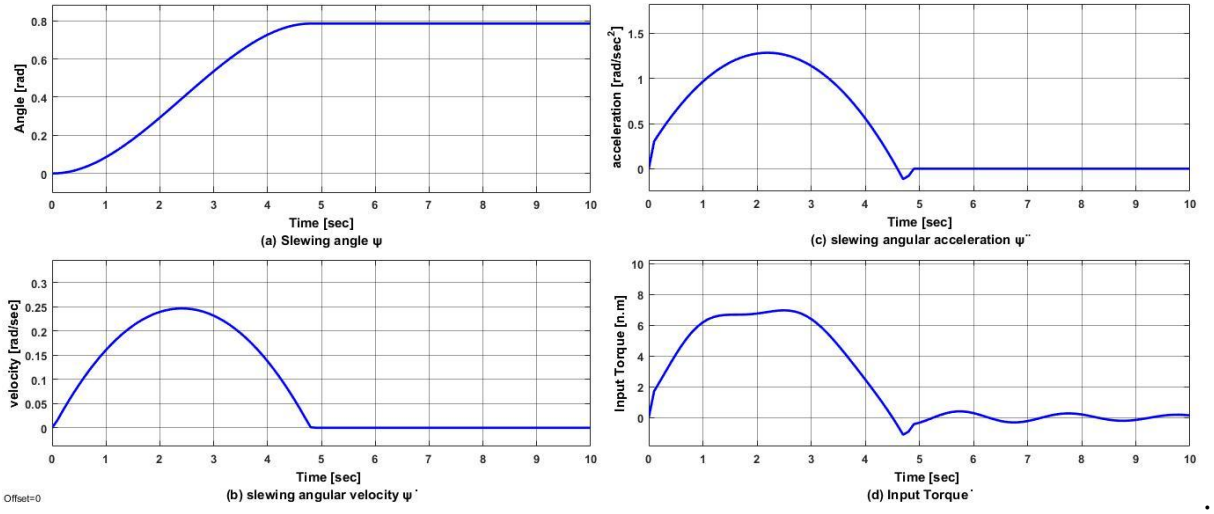

Fig. 2. Cubic Polynomial trajectory with ψ_f=45 [deg] (ψ_f=0.7853[rad])

3.2. Quantic Polynomial Trajectory

Forcing the trajectory to have specific position, velocity, and acceleration at boundaries introduces six constrains, so a fifth order polynomial is needed to define position as following

$$\psi(t) = a_0 + a_1 t + a_2 t^2 + a_3 t^3 + a_4 t^4 + a_5 t^5 \tag{22}$$

Then the velocity and acceleration are derived as follows:

$$\dot{\psi}(t) = a_1 + 2a_2 t + 3a_3 t^2 + 4a_4 t^3 + 5a_5 t^4 \tag{23}$$

$$\ddot{\psi}(t) = 2a_2 + 6a_3 t + 12a_4 t^2 + 20a_5 t^3 \tag{24}$$

Values of $(a_0, a_1, a_2, a_3, a_4, a_5)$ can be determined from the boundary conditions, where the shape of the trajectory(position, velocity, acceleration) curves of a quantic path starts at t_0=0 sec with ψ_0=0 [deg] , $\dot{\psi}_0$=0 [deg/sec] and $\ddot{\psi}_0$=0 [deg/sec^2] (initial slewing angle, initial velocity and acceleration respectively), and ends at t_f=10 [sec] with ψ_f=45 [deg] (ψ_f=0.7853[rad]), $\dot{\psi}_f$=0 [deg/sec] and $\ddot{\psi}_f$=0 [deg/sec^2] (final slewing angle, final velocity and acceleration respectively) as shown in Fig. 2.

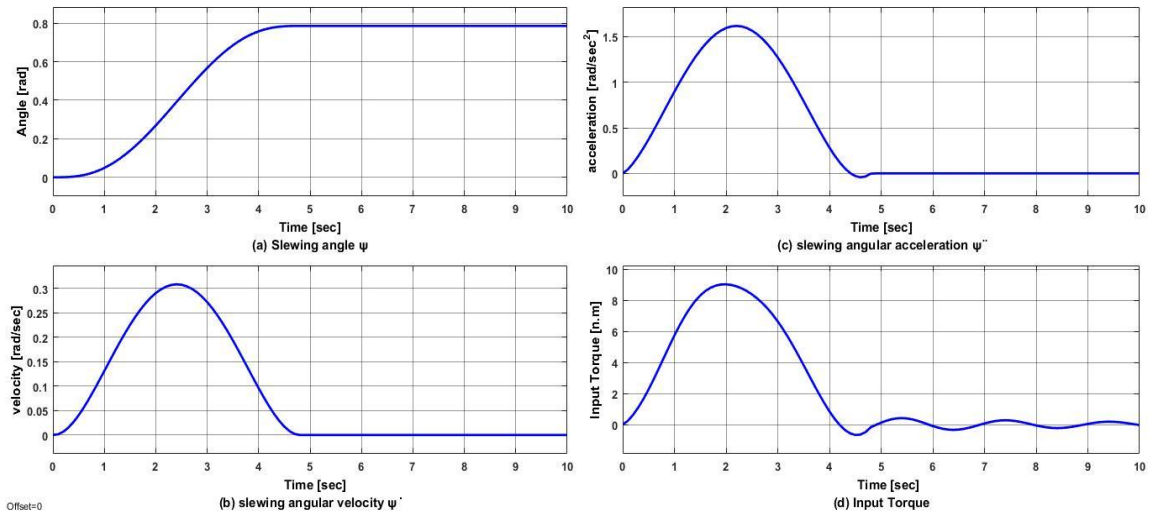

Fig. 2. Quantic Polynomial trajectory with ψ_f=45 [deg] (ψ_f=0.7853[rad])

3.3. Zero Jerks Trajectory

To make a trajectory start and stop with zero jerks, a polynomial of seventh degree is needed to present position.

$$\psi(t) = a_0 + a_1 t + a_2 t^2 + a_3 t^3 + a_4 t^4 + a_5 t^5 + a_6 t^6 + a_7 t^7 \tag{11}$$

Therefore, the velocity, acceleration, and jerk are presented as following:

$$\dot{\psi}(t) = a_1 + 2a_2 t + 3a_3 t^2 + 4a_4 t^3 + 5a_5 t^4 + 6a_6 t^5 + 7a_7 t^6 \tag{11}$$

$$\ddot{\psi}(t) = 2a_2 + 6a_3 t + 12a_4 t^2 + 20a_5 t^3 + 30a_6 t^4 + 42a_7 t^5 \tag{11}$$

$$\dddot{\psi}(t) = 6a_3 + 24a_4 t + 60a_5 t^2 + 120a_6 t^3 + 210a_7 t^4 \tag{11}$$

Values of $(a_0, a_1, a_2, a_3, a_4, a_5, a_6, a_7)$ can be determined from the boundary conditions, where the shape of the trajectory(position, velocity, acceleration and jerk) curves of a zero jerk path starts at t_0=0 sec with ψ_0=0 [deg] , $\dot{\psi}_0$=0 [deg/sec] and $\ddot{\psi}_0$=0 [deg/sec²] (initial slewing angle, initial velocity and acceleration respectively), and ends at t_f=10 [sec] with ψ_f=45 [deg] (ψ_f=0.7853[rad]), $\dot{\psi}_f$=0 [deg/sec] and $\ddot{\psi}_f$=0 [deg/sec²] (final slewing angle, final velocity and acceleration respectively) $\dddot{\psi}_0$=0 [deg/sec^3] and $\dddot{\psi}_f$=0 [deg/sec^3] (initial and final jerk respectively) as shown in Fig. 3.

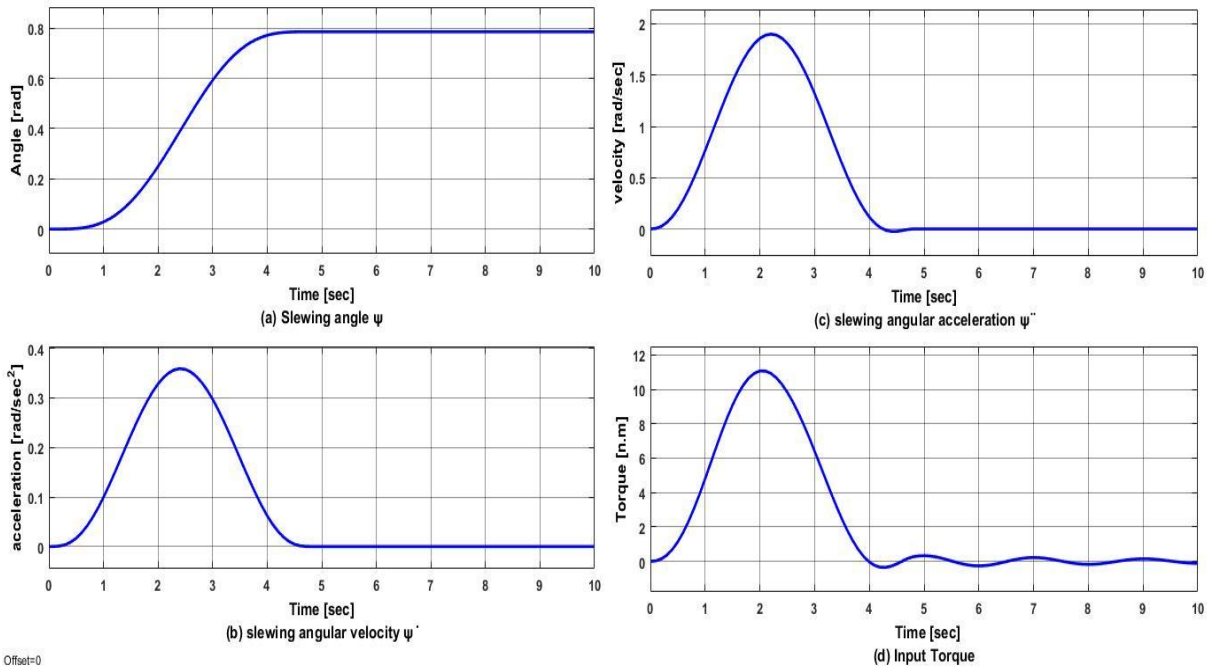

Fig. 3. Zero jerk trajectory with ψ_f=45 [deg] (ψ_f=0.7853[rad])

3.4. S-Curve Trajectory

In this section, we present a method which used in [6] for generating the S-curve trajectory for slewing rotational boom motion that can suppress residual load sway by the following reference:

$$r=\begin{cases} \mathrm{At}(1-\dfrac{1}{\pi/t_1}\sin(\dfrac{\pi}{t_1}t)) & t\in[0,t_1] \\ A(2t-t_1) & t\in[t_1,t_1+t_2] \\ \mathrm{A}(\mathrm{t}+\dfrac{1}{\pi/t_3}\sin(\dfrac{\pi}{t_3}t')+t_2) & t\in[t_1+t_2,t_1+t_2+t_3] \\ \psi_f & t\in[t_1+t_2+t_3,t_f] \end{cases} \tag{11}$$

where ψ_f and t_f are the final angle and the final time, respectively. In this study, we set t_f=10 [sec] and take the same parameters and trajectory conditions used in [8] to be compared later, which as follows:

Table 1 Trajectory generation conditions and results [ ]

	ψ_f=45 [deg]	ψ_f=35 [deg]	ψ_f=55 [deg]
$\dot{\psi}_c$[rad/s].	0.273	0.212	0.333
t_1[sec]	1.903	1.903	1.903
t_2[sec]	0.907	0.907	0.907
t_3[sec]	1.903	1.903	1.903

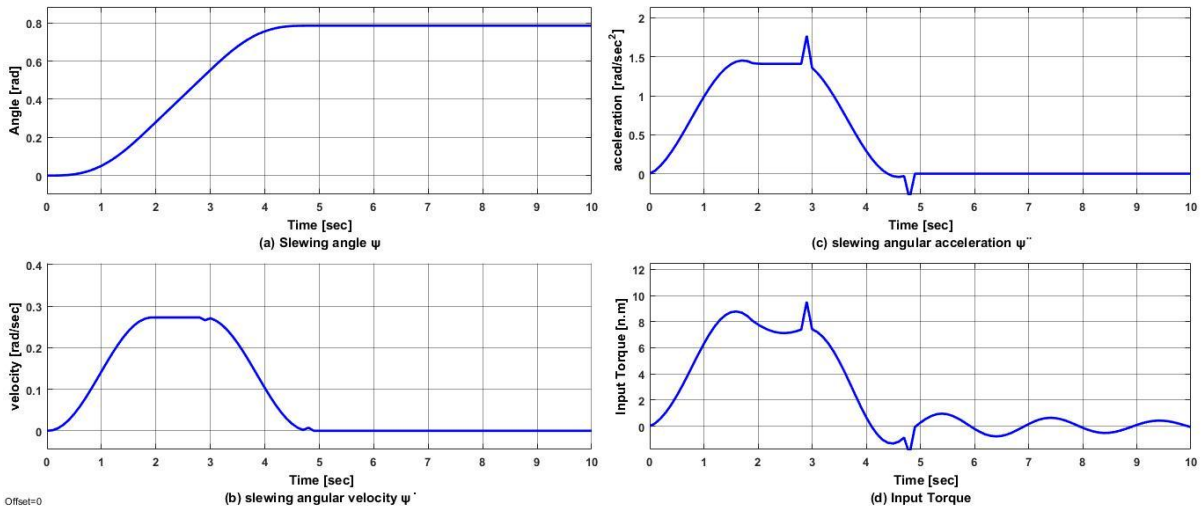

Fig. 4 S-curve trajectory with ψ_f=45 [deg] (ψ_f=0.7853[rad])

4. Results and Discussion

This section presents the efficiency of TRC model and the Sim-Mechanics model by applying different reference trajectories and different inputs such as (damping ratio ,friction coefficient ,vertical boom angle,…etc.) to our Sim-Mechanics model and compare the results of the two swaying angles with the difference inputs. Because Eqs. (17) and (18) are nonlinear and it is difficult to be solved analytically to predict the value of the swaying angles, so the Sim-Mechanics model will be more effective to compute and predict the swaying angle and the sensing with the computed torque, which need from the slewing motor to reach the target point. On the other hand, the simple model will be useful to apply different types of control on our Sim-mechanics model to calculate the controller gains easily for feedback control.

The initial conditions and results for trajectory generation on the basics of the proposed method in Eqs. (17) and (18) are nonlinear, numerical solutions depend on their initial values have to be solved as these are only algebraic Eqs. (20)-(33), not differential equations, in the proposed method, a discretization procedure as well as iterative calculation with respect to time variable is not required. One of the main advantages of the proposed model is simple required computation the possibility of obtaining the solution is increased. First, the generated cubic trajectory is applied and generate a smooth curve as shown in Fig.12.

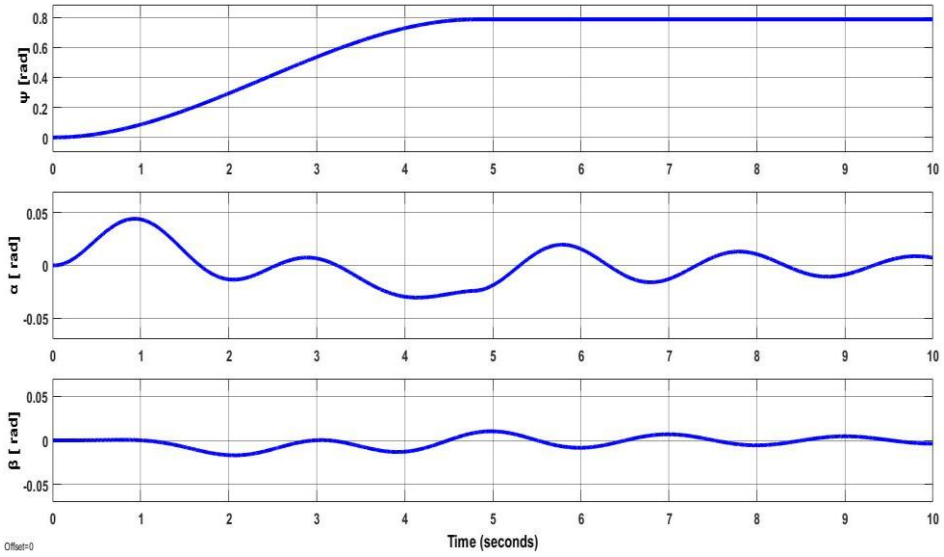

Fig. 12 Cubic polynomial method with ψ=45 [deg]

Then quadratic path trajectory is introduced because all points on the position and velocity curves continuous with time, but acceleration is discontinuous as acceleration constrains do not present in this path. Derivative of acceleration is called the jerk. A discontinuity in acceleration leads to an impulsive jerk, which may excite vibration modes and the simulation results are shown in Fig.13.

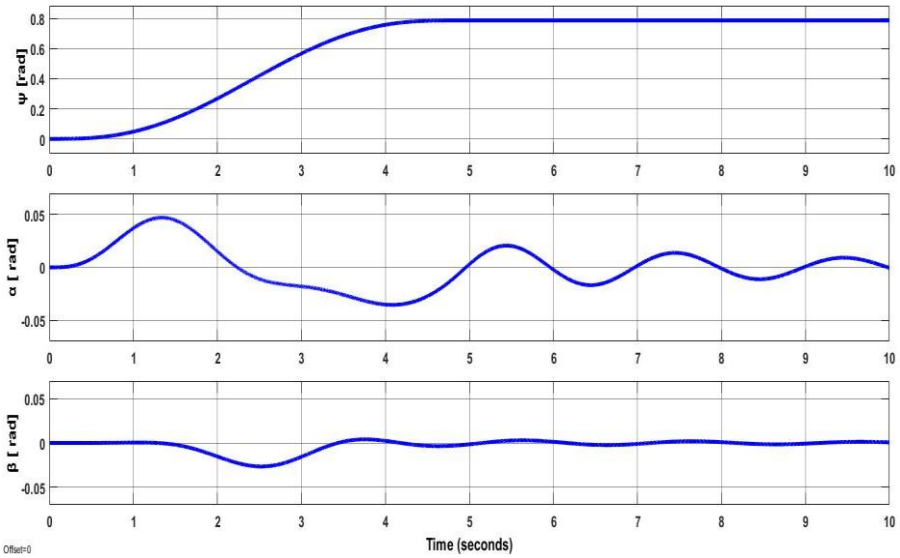

Fig. 13 Quantic polynomial method with ψ=45 [deg]

The results of applying the reference quantic trajectory is better than that of cubic path trajectory as there are more damping of oscillation of swaying angles because of the acceleration and deceleration at the start and end points equal to zero

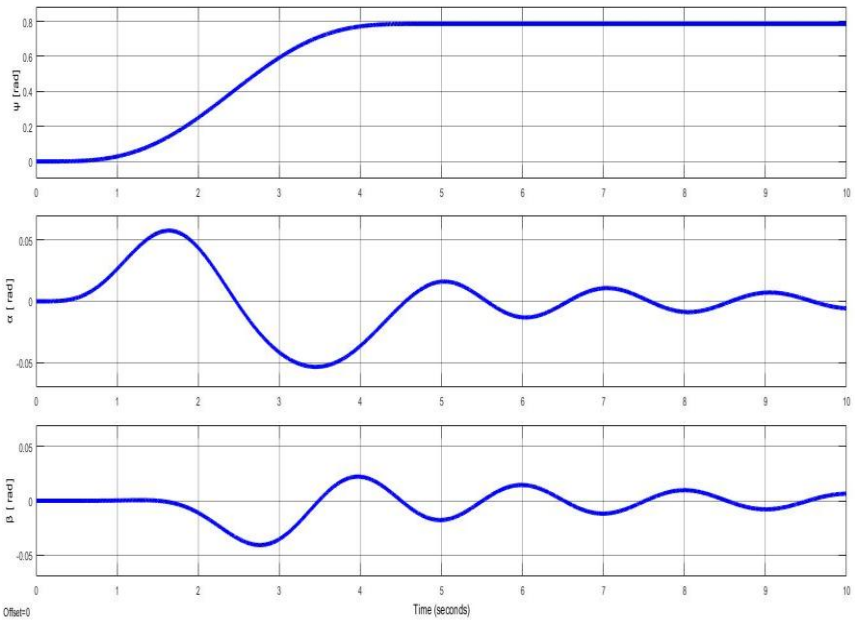

Fig. 14 Zero Jerk polynomial method with ψ=45[deg]

So higher order polynomial needs to be used to include acceleration constrains in addition and to make a trajectory start and stop with zero jerks, a polynomial of seventh degree is needed to present position simulation results are shown in Fig.14, The residual load sway is suppressed completely as shown in Fig. 14 while the boom tracks the reference trajectory.
These results confirm the effectiveness of our proposed trajectory generation method for the assumed simplified model.

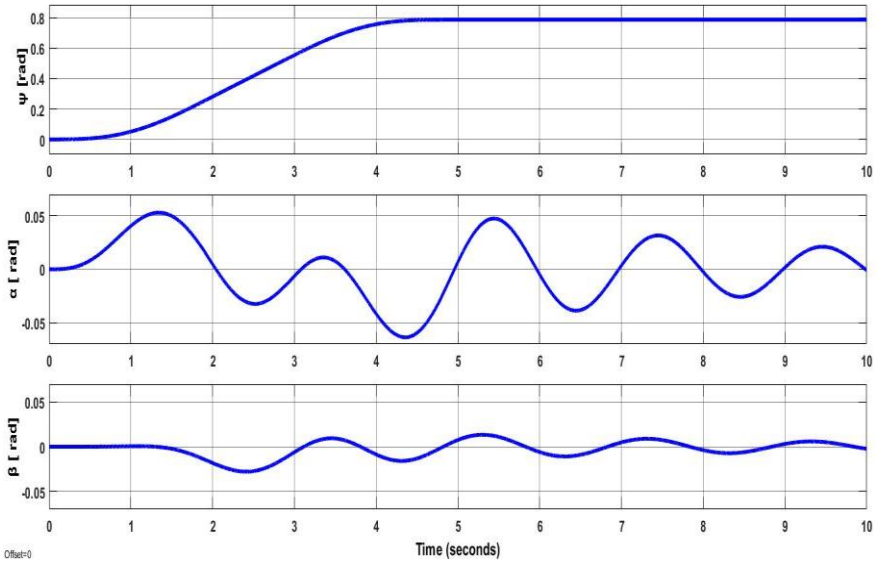

Fig. 15 S-curve trajectory generation method with ψ=45[deg]

An additional S-curve trajectory used in ref. [6] have applied to (Sim-Mechanics model),.Simulation results are shown in Fig. 15. Which its results is near from that of zero jerk one so a comparative between the two trajectory is shown in Fig 16

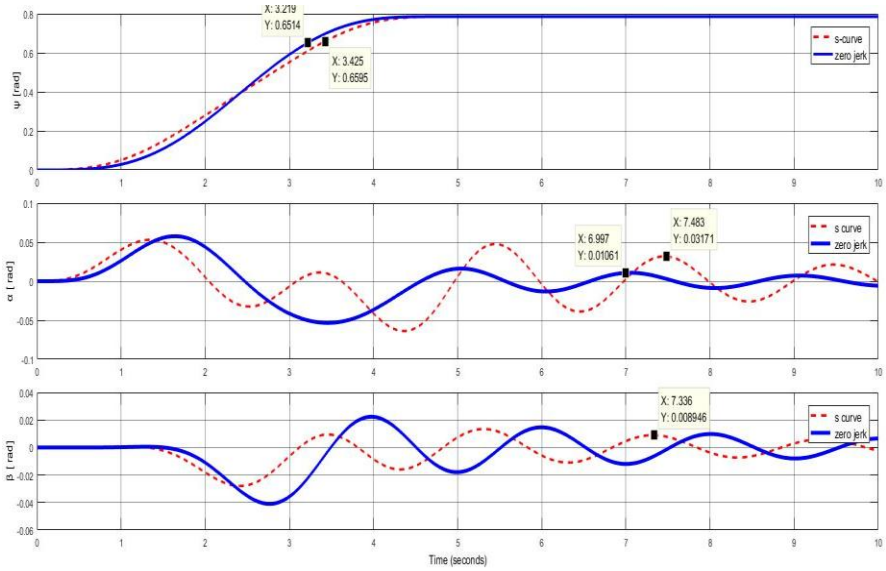

Fig. 16 S_curve with Zero jerk method with ψ=45[deg]

The trajectory method and the method used in [6] applied to the same model at SimMechanics to validate the effectiveness of our proposed method in comparison with the other method and the results are shown in Fig. 16. The maximal amplitude of residual load sway as shown in Fig.

14 is decreased about 45% from that shown in Fig. 12,13and15, while almost the same performance of residual load sway suppression are obtained in Figs. 15 and 16.
To demonstrate the effect of the friction between the rope and the top of the boom, WE consider the following viscous friction term in the left-hand side of Eq. (13) $f_{v\theta_1} = c_{\theta_1}\dot{\theta}_1$ where, $c_{\theta_1}$is the viscous friction coefficient.
By applying classical PD control to our system, the results are shown in Fig. 17. The PD feedback gains are determined by an LMI based method described in [19] Because this control system feedbacks the load sway signals and uses both horizontal and vertical boom motion to suppress the load sway, shorter control time with small residual load sway is achieved. However, it can be confirmed that the proposed approach provides comparable performance as in Fig. 14, though it does not use load sway signals and employs only trajectory generation

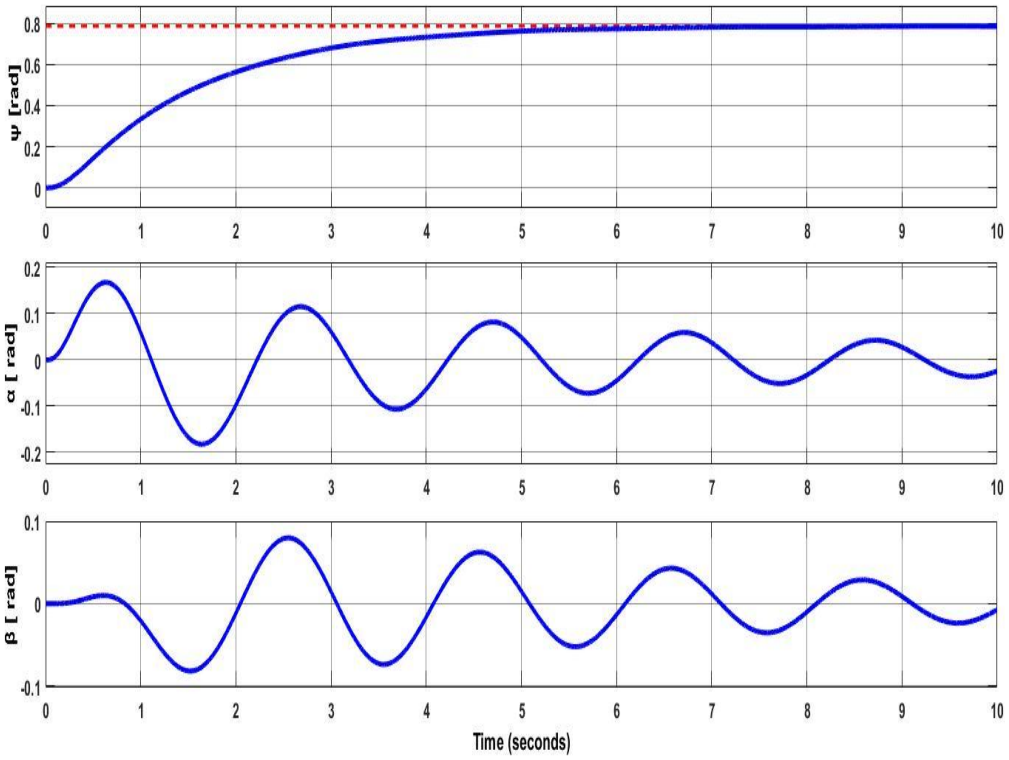

Fig. 16 classical PD control method with ψ=45[deg]

6. Conclusion and Future Work

Our objective is to build a model for the telescopic rotary crane (TRC) that can predict the values of the swaying angles to use it as a feedback signal to suppress the residual load sway as possible by using different control methods
The validation of the model achieved by applying different reference trajectories and different inputs such as (damping ratio, friction coefficient, vertical boom angle…etc.) to Sim-Mechanics model and compare the results of the two swaying angles with the different inputs.
Next, the conditions for trajectory generation (an S-curve trajectory, cubic trajectory, quantic trajectory and zero jerks trajectory) of horizontal boom motion are considered to suppress residual load sway. The trajectory parameters that suppress the residual load sway can be obtained numerically by solving only algebraic equations. The effectiveness of the proposed simple model of crane and trajectory was verified by numerical simulations and 3D virtual results using SimMechanics toolbox
One of advantages of the proposed model is the simple computation needed. Another advantages of the proposed model is its applicability on the rotor cranes, whose research is few attempted in literature

Future work includes developing a control strategy depending on simulation results to suppress the load sway during loading /unloading operations, applying these results experimentally with considering this safety problem. The rope length variance should be considered as well.

7. References

[1] Y. Sakawa and Y. Shindo, "Optimal control of container cranes," *Automatica*, vol. 18, pp. 257-266, 1982.

[2] Y. Sakawa and A. Nakazumi, "Modeling and control of a rotary crane," *Journal of Dynamic Systems, Measurement, and Control*, vol. 107, pp. 200-206, 1985.

[3] K. Terashima, Y. Shen, and K. i. Yano, "Modeling and optimal control of a rotary crane using the straight transfer transformation method," *Control Engineering Practice*, vol. 15, pp. 1179-1192, 2007.

[4] K. A. Moustafa, "Reference trajectory tracking of overhead cranes," *Journal of Dynamic Systems, Measurement, and Control*, vol. 123, pp. 139-141, 2001.

[5] H.-H. Lee, "A new motion-planning scheme for overhead cranes with high-speed hoisting," *TRANSACTIONS-AMERICAN SOCIETY OF MECHANICAL ENGINEERS JOURNAL OF DYNAMIC SYSTEMS MEASUREMENT AND CONTROL*, vol. 126, pp. 359-364, 2004.

[6] N. Uchiyama, H. Ouyang, and S. Sano, "Simple rotary crane dynamics modeling and open-loop control for residual load sway suppression by only horizontal boom motion," *Mechatronics*, vol. 23, pp. 1223-1236, 2013.

[7] M. A. Ahmad, M. S. Ramli, R. M. T. R. Ismail, and R. E. Samin, "Trajectory Control and Sway Suppression of a Rotary Crane System," in *Machine Vision and Mechatronics in Practice*, ed: Springer, 2015, pp. 165-175.

[8] N. Uchiyama, S. Sano, and H. Ouyang, "Simple Dynamics and Open-Loop Control for Horizontal Boom Motion of Rotary Cranes," in *ASME 2014 International Manufacturing Science and Engineering Conference collocated with the JSME 2014 International Conference on Materials and Processing and the 42nd North American Manufacturing Research Conference*, 2014, pp. V001T04A036-V001T04A036.

[9] N. Sun and Y. Fang, "An efficient online trajectory generating method for underactuated crane systems," *International Journal of Robust and Nonlinear Control*, vol. 24, pp. 1653-1663, 2014.

[10] S.-J. Kimmerle, M. Gerdts, and R. Herzog, "Optimal control of an elastic crane-trolley-load system–A case study for optimal control of coupled ODE-PDE," 2015.

[11] S.-J. Kimmerle, M. Gerdts, and R. Herzog, "Optimal control of an elastic crane-trolley-load system–A prototype for optimal control of coupled ODE-PDE," 2013.

[12] W. Devesse, M. Ramteen, L. Feng, and J. Wikander, "A real-time optimal control method for swing-free tower crane motions," in *2013 IEEE International Conference on Automation Science and Engineering (CASE)*, 2013, pp. 336-341.

[13] W. Devesse, "Slew control methods for tower cranes," 2012.

[14] Z. N. Masoud, N. A. Nayfeh, and A. H. Nayfeh, "Sway reduction on container cranes using delayed feedback controller: Simulations and experiments," in *ASME 2003 International Design Engineering Technical Conferences and Computers and Information in Engineering Conference*, 2003, pp. 2221-2229.

[15] J. Neupert, E. Arnold, K. Schneider, and O. Sawodny, "Tracking and anti-sway control for boom cranes," *Control Engineering Practice*, vol. 18, pp. 31-44, 2010.

[16] F. Piltan, S. Emamzadeh, Z. Hivand, F. Shahriyari, and M. Mirazaei, "PUMA-560 Robot Manipulator Position Sliding Mode Control Methods Using MATLAB/SIMULINK and Their Integration into Graduate/Undergraduate Nonlinear Control, Robotics and MATLAB Courses," *International Journal of Robotics and Automation*, vol. 3, pp. 106-150, 2012.

[17] F. Piltan, M. H. Yarmahmoudi, M. Shamsodini, E. Mazlomian, and A. Hosainpour, "PUMA-560 Robot Manipulator Position Computed Torque Control Methods Using MATLAB/SIMULINK and Their Integration into Graduate Nonlinear Control and MATLAB Courses," *International Journal of Robotics and Automation*, pp. 167-191, 2012.

[18] J. J. Craig, *Introduction to robotics: mechanics and control* vol. 3: Pearson Prentice Hall Upper Saddle River, 2005.

[19] S. Shigenori, H. Ouyang, H. Yamashita, and N. Uchiyama, "LMI approach to robust control of rotary cranes under load sway frequency variance," *Journal of System Design and Dynamics*, vol. 5, pp. 1402-1417, 2011.